

Transport properties of Methane, Ethane, Propane, and n-Butane in Water

Sunil Pokharel,^{1,*} Narayan Aryal,^{1,†} Bhakta Raj Niraula,^{1,‡}
Arjun Subedi,^{1,§} and Narayan Prasad Adhikari^{1,¶}

¹*Central Department of Physics, Tribhuvan University, Kirtipur, Kathmandu, Nepal*

(Dated: October 18, 2017)

In this work, we have estimated self diffusion coefficients along with the binary diffusion coefficients of mixtures of alkane (methane, ethane, propane and n-butane) in SPC/E water(H₂O). Molecular dynamics study of a binary mixture of alkane gas and SPC/E water, with alkane as solute and water as solvent, have been carried out at different temperatures ranging from 283.15 K to 333.15 K. We have taken a dilute solution of 3 alkane (methane, ethane, propane and n-butane) molecules and 971 water molecules in a system. The role of interaction in the structure of the constituents of the system as a function of temperature is studied with the help of the radial distribution function (RDF) and the coordination numbers. The self-diffusion coefficient of the constituents of the mixture was calculated by using mean square displacement (MSD) and the binary diffusion coefficients of alkane in water have been calculated by using Darken's relation. The results are then compared with the available experimental values. The values of self-diffusion coefficients of water from the present work come in good agreement with the experimental values within 9% error. The binary diffusion coefficients of ethane, methane, propane and n-butane agree with the previously reported experimental values. The dependence of the diffusion coefficients on temperature is approximated by Arrhenius-type exponential relationship.

Keywords: Alkane, Diffusion Coefficient, Molecular dynamics, Coordination numbers, Arrhenius behavior

I. INTRODUCTION

Alkanes are saturated hydrocarbons that consist only of the elements carbon (C) and hydrogen (H), where each of these atoms are linked together exclusively by single bonds. Alkanes belong to a homologous series of organic compounds in which the members differ by a constant molecular mass of 14 that is CH₂¹. The smaller members of the alkane family are gases, while the larger are liquid and solid compounds. The alkanes are soluble in non-polar solvents such as benzene, ether and chloroform, and are insoluble in water and other highly polar solvents. The most important sources of alkanes are natural gas and crude oil. Petroleum and natural gas are largely mixtures of different alkanes. On refining, they give liquefied petroleum gas (LPG), gasoline, kerosene, diesel, furnace oil and wax which are used as fuels. The solid alkanes (compounds) are typically waxy in texture. The uses of alkanes can be determined according to the number of carbon atoms present in it. Some of the common uses of alkanes are heating, electricity generation, cooking, production of polymers, serves as intermediate in the synthesis of drugs, pesticides and other chemicals, components of gasoline (pentane and octane) and paraffin wax. First four members of alkane series are methane, ethane, propane, and butane with molecular formula CH₄, C₂H₆, C₃H₈, and C₄H₁₀ re-

spectively. The first four alkanes are used for heating, cooking and electricity generation. The main components of natural gas are methane and ethane. Propane and Butane are used as LPG (liquefied petroleum gas). Propane is also used in the propane gas burner, butane in disposable cigarette lighters. They are also used as propellants in aerosol sprays. The processing of natural gas involves removal of propane, butane, and large amount of ethane from the raw gas in order to prevent condensation of these volatiles in natural gas pipelines Alkanes have a number of industrial applications beyond fuels, including uses in cosmetics and plastics. Alkanes are generally less reactive than alkenes and alkynes because they lack the more reactive double and triple bonds. However, they do participate in reactions with oxygen (combustion) and halogens¹⁻⁴. Modeling and Computer simulation are carried out in the hope of understanding the properties of assemblies of molecules in terms of their structure and the microscopic interactions between them. This serves as a complement to conventional experiments, enabling us to learn something new, something that cannot be found out in other ways⁵⁻¹⁰. The two main families of computer simulation technique are molecular dynamics (MD) and Monte Carlo (MC); additionally, there is a whole range of hybrid techniques which combine features from both. The obvious advantage of MD over MC is that it gives a route to dynamical properties of the system: trans-

port coefficients, time-dependent responses to perturbations, rheological properties and spectra^{5,6}. Molecular Dynamics simulation is a technique for computing the equilibrium and transport properties of a classical many-body system. In this context, the word classical means that the nuclear motion of the constituent particles obeys the laws of classical mechanics. This is an excellent approximation for a wide range of materials. Molecular dynamics simulation consists of the numerical, step-by-step, solution of the classical equations of motion^{5,6}

$$m_i \frac{d^2 \mathbf{r}_i}{dt^2} = \mathbf{F}_i = -\nabla_{\mathbf{r}_i} U \quad (1)$$

For this purpose we need to be able to calculate the forces \mathbf{F}_i acting on the atoms, and these are usually derived from a potential energy $U(\mathbf{r}^N)$, where $\mathbf{r}^N = (\mathbf{r}_1, \mathbf{r}_2, \dots, \mathbf{r}_N)$ represents the complete set of $3N$ atomic coordinates.

As different species of a mixture move under the influence of concentration inhomogeneity, molecular diffusion occurs¹¹. It plays a vital role in variety of biospheric and atmospheric sciences. Diffusion is basic for transport of matter and for ionic conduction in disordered materials^{12,13}. The kinetics of many micro structural changes that occur during preparation, processing and heat treatment of materials include diffusion. The typical examples are nucleation of new phases, diffusive phase transformation, precipitation and dissolution of a second phase, homogenization of alloys, recrystallization and thermal oxidation¹¹. Alkanes are less reactive in comparison to other chemical species because carbon atoms in alkanes have attained their octet of electrons through forming four covalent bonds. These four bonds formed by carbon in alkanes are called sigma bonds, which are more stable than other types of bond because of the greater overlaps of carbons atomic orbitals with the neighbouring atoms atomic orbitals. Alkanes are non-polar solvents as only C and H atoms are present. Alkanes are insoluble in polar solvent like water but freely soluble in non-polar solvent like ether and benzene. Since alkanes are rarely soluble in water, it is very appropriate and interesting to study the diffusion of alkane in water. The first four members of alkane series exist in the vapour state under the normal atmospheric condition, which are principle ingredients in natural gas. Melting point and boiling point of alkanes increase with the increase in number of carbon atoms. The principle source of alkanes is petroleum, which consists together with the accompanying natural gas. The complicated organic compounds that once made up living plants or animals have transformed into a mixture of alkanes

ranging in size from one carbon to 30 or 40 carbons by decay and millions of years of geological stresses¹.

It is found that the diffusion of hydrocarbons (alkanes) in water is a basic consideration in many processes like processing of natural gases and petroleum, understanding the tertiary structure of proteins, as well as the important role it plays as a driving force in a number of processes occurring within living cells. The experimental values of binary diffusion coefficients of alkane-water mixture have been obtained by D. L. Wise and G. Houghton by using the rate of collapse of small bubbles in gas free water¹⁴. Also, P. A. Witherspoon and D. N. Saraf have been obtained by using the capillary cell method¹⁵. The result of both techniques are different. Figure (1) shows the plot of the binary diffusion coefficients of the two experimental works. The value of binary diffusion coefficients from¹⁴ are deviated at most 76 % than that of¹⁵. Such discrepancies in these works motivated us to carry out a computational work to study the diffusion phenomena of alkane in water. Our results obtained from simulation also can be used as a crude reference for any further studies of diffusion in complex fluid mixtures and improve our understanding of hydrocarbons and other more complex biological macromolecules like protein in water¹⁶.

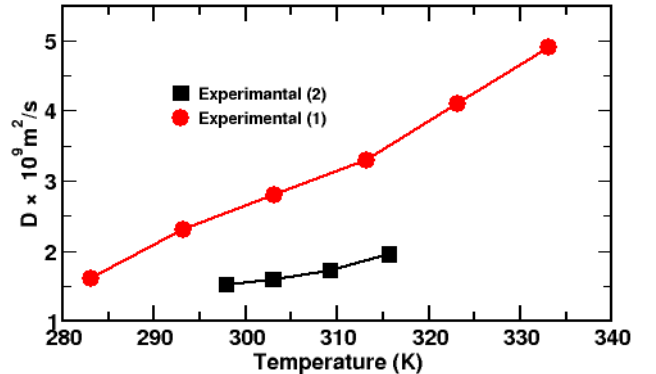


FIG. 1. Plot of binary diffusion coefficient of ethane-water system versus temperature of two experimental works^{14,15}

The outline of the paper is as follows: In Sec. II, we discuss the theory of diffusion and method of calculation of diffusion coefficient. Computational details of our work are stated in Sec. III. Results of our work are presented in Secs. IV. Our conclusions are collected in Sec. V.

II. DIFFUSION COEFFICIENT

Diffusion is the process by which matter is transported from one part of the system with higher concentration to the another part of the system with the lower concentration as a result of random molecular motion. The driving force of diffusion is thermal motion of the molecules. The higher concentration of a species in a system at a particular site corresponds to its higher value of chemical potential. The net transport of the mass takes place from the region of higher chemical potential to the region of lower chemical potential. At the end of such net transport, the system attains a situation where there exists same value of chemical potential in the system. In this situation, free energy of the system is minimum and hence its entropy becomes maximum; system is at dynamic equilibrium¹⁷. The response property of a system to a concentration gradient is measured by diffusion coefficient⁵. The diffusion in a homogeneous system where no chemical concentration gradient exists is known as self-diffusion and the corresponding diffusion coefficient is called self-diffusion coefficient¹⁸. There are two common ways to obtain a self-diffusion coefficient. The mathematical expression to calculate self-diffusion coefficient from molecular positions is famously known as Einstein relation^{5,6}. For 3-D system,

$$D = \lim_{t \rightarrow \infty} \frac{\langle [\mathbf{r}_\alpha(t + t_0) - \mathbf{r}_\alpha(t_0)]^2 \rangle}{6t} \quad (2)$$

where α denotes the type of component (solute or solvent) and t_0 is any time origin. The angled brackets $\langle \dots \rangle$ indicate the ensemble average. The ensemble average is taken over all atoms of the component α in the simulation and all time origins¹⁹. The method using Einstein relation for calculating diffusion coefficients is known as MSD method.

In this work, we calculate the self diffusion coefficients of both the components i.e. alkane (methane, ethane, propane, n-butane) and water (H₂O) which can be used to estimate the binary diffusion coefficient using Darken's relation²⁰

$$D_{AB} = N_B D_A + N_A D_B \quad (3)$$

where D_A , D_B are the self diffusion coefficients of species A and B respectively and N_A , N_B are the corresponding mole fractions.

III. COMPUTATIONAL DETAILS

A. Molecular Models

The SPC/E (simple point charge/extended) potential model²¹ is used in all the simulation for water as a solvent. The OPLSS-AA (Optimized Potentials for Liquid Simulations-All Atom) potential model²² is used for alkanes (methane, ethane, propane, n-butane) as solute. The system under study consists of 3 alkane (methane, ethane, propane, n-butane) molecules and 971 water molecules separately. In classical force fields like OPLS-AA, the potential functions are derived empirically to describe the atomic interactions. The atoms are treated as spherically symmetric particles and are considered to be connected through covalent bonds to form molecules. Each and every atom experiences a force resulting from its pairwise additive interactions with the rest of the system. The total potential energy U_{tot} includes contributions from both bonded and non-bonded interactions²³. The bonded interactions are bond stretching (2-body), bond angle (3-body) and dihedral angle (4-body) interactions. A special type of dihedral interaction (called improper dihedrals) is used to force atoms to remain in a plane or to prevent transition to a configuration of opposite chirality (a mirror image). The non-bonded interactions are represented by the van der Waals potential and Coulomb potential. Therefore, the total potential energy function of a system can be written as as²³:

$$U_{\text{tot}} = U_b + U_{\text{nb}} \quad (4)$$

$$U_{\text{tot}} = U_b + U_a + U_d + U_{\text{id}} + U_{\text{vdw}} + U_c \quad (5)$$

The bond stretching between two covalently bonded atoms i and j is represented by harmonic potential²³

$$U_b(r_{ij}) = \frac{1}{2} k_{ij}^b (r_{ij} - b_{ij})^2 \quad (6)$$

where k_{ij}^b is the force constant and b_{ij} is the equilibrium bond length between two atoms i and j . The bond angle vibration between a triplet of atoms $i - j - k$ is also represented by a harmonic potential on the angle Θ_{ijk} ²³

$$U_a(\Theta_{ijk}) = \frac{1}{2} k_{ijk}^\Theta (\Theta_{ijk} - \Theta_{ijk}^0)^2 \quad (7)$$

where k_{ijk}^Θ is the force constant and Θ_{ijk}^0 is the equilibrium bond angle.

The proper dihedral angle is defined by the angle between the ijk and jkl . The periodic dihedral potential is defined by²³ :

$$U_d = k_{ijkl}^\phi (1 + \text{Cos}(n_{ijkl} \phi_{ijkl} - \phi_0)) \quad (8)$$

Here ϕ_{ijkl} is dihedral angle, k_{ijkl}^ϕ is the the force constant, ϕ_0 is the reference angle where the potential passes through its minimum value, and n_{ijkl} is the multiplicity, which indicates the number of minima as the bond is rotated through 2π . The multiplicity is a nonzero, positive integer number.

For alkanes, the following proper dihedral potential (Ryckaert-Bellmans function) is often used²³:

$$U_{rb} = \sum_{n=0}^5 C_n (\text{Cos}(\psi))^n \quad (9)$$

where $\psi = \phi - 180^\circ$.

The improper dihedral potential is harmonic potential which is given by²³:

$$U_{id} = \frac{1}{2} k_\xi (\xi_{ijkl} - \xi_0)^2 \quad (10)$$

where the parameters ξ_0 and k_ξ mark the equilibrium improper dihedral angle and force constant respectively.

The non-bonded interatomic interaction is the sum of Lennard- Jones interaction and Coulomb interaction. The interatomic interaction thus can be written as

$$U_{\alpha\beta}(r_{ij}) = 4\epsilon_{\alpha\beta} \left[\left(\frac{\sigma_{\alpha\beta}}{r_{ij}} \right)^{12} - \left(\frac{\sigma_{\alpha\beta}}{r_{ij}} \right)^6 \right] + \frac{q_{i\alpha} q_{j\beta}}{4\pi\epsilon_0 r_{ij}} \quad (11)$$

where r_{ij} is the Cartesian distance between the two atoms i and j ; α and β indicate the type of the atoms. The parameters for the non-bonded Lennard Jones interaction between two different atoms for OPLS-AA force field are written as²³:

$$\sigma_{\alpha\beta} = (\sigma_{\alpha\alpha} \times \sigma_{\beta\beta})^{\frac{1}{2}} \quad (12)$$

$$\epsilon_{\alpha\beta} = (\epsilon_{\alpha\alpha} \times \epsilon_{\beta\beta})^{\frac{1}{2}} \quad (13)$$

B. Simulation Set up

MD simulation was carried out in a cubic box with periodic boundary conditions⁶ using **GROMACS 4.6.5**. The distance to the edge of the box from the solute (alkane) is an important parameter for defining the size of the box. Since we are using periodic boundary conditions, we must satisfy the minimum image convention. That is alkane (solute) should never see its periodic image, otherwise the forces calculated will be spurious. The size of the box defined here is sufficient for just about any cutoff scheme commonly used in simulations. After solvation, addition of 971 water molecules and 3 alkanes molecules in simulation box, energy minimization is

carried out with a cut off restriction of 1.0 nm to avoid unphysical van der Waals contact caused by the atoms that are too close²³. Energy minimization brings the system to equilibrium configuration, removes all the kinetic energy from the system, reduces thermal noise in structure and brings the system to one of the local minimum. Steepest descent algorithm has been used for energy minimization and the algorithm stops when the maximum of absolute value of force components is smaller than the specified value²³. The energy (potential) of the system after energy minimization is shown in figure (2).

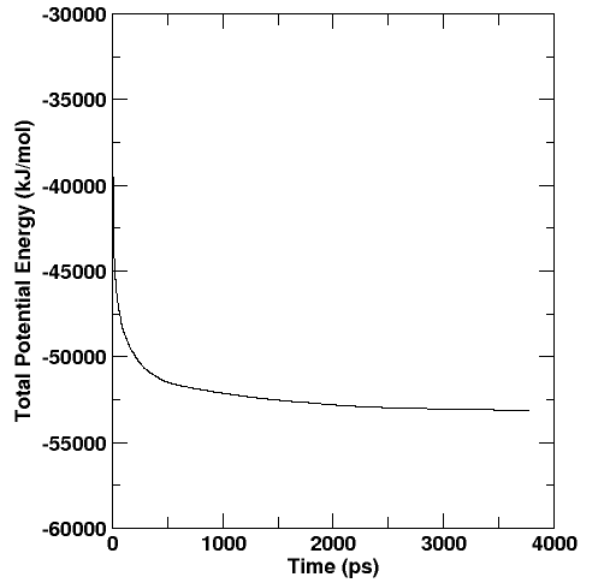


FIG. 2. Plot of potential energy as a function of time after energy minimization for methane-water system.

After energy minimization, equilibrium was carried out at different temperatures, 283.15 K, 293.15 K, 303.15 K, 313.15 K, 323.15 K, 333.15 K and a pressure of 10^5 Nm^{-2} (i.e. NPT Ensemble) by using *velocity-rescaling* thermostat and Berendsen barostat²³ at a coupling time $\tau_t = 0.01 \text{ ps}$ and $\tau_p = 0.8 \text{ ps}$ respectively. Here, the system is subjected to NPT ensemble to bring the parameters like temperature, pressure, density, etc. to thermodynamic equilibrium because dynamic property like diffusion coefficient varies with such parameters. We used MD integrator with time step size 0.002 ps for 10^9 steps, which makes equilibration run of 200 ns. The velocity is generated initially according to a Maxwell distribution function at a specified temperature²³. All the bonds are converted to constraints using SHAKE algorithm²³. During equilibration short range coulomb interaction and Lennard Jones interaction each with a cut off parameter of 1.0 nm were

considered with periodic boundary conditions⁶. The long range Coulomb interaction is handled via the PME (Particle Mesh Ewald) algorithm with fourier spacing 0.12. The input parameters (force field parameters, and coupling constants for barostat and thermostat) were taken so as to be consistent with the experimental values as much as possible. The structure of the system after equilibration is shown in figure(3). The density and simulated temperatures at different coupling temperatures for propane in water are shown in table (I).

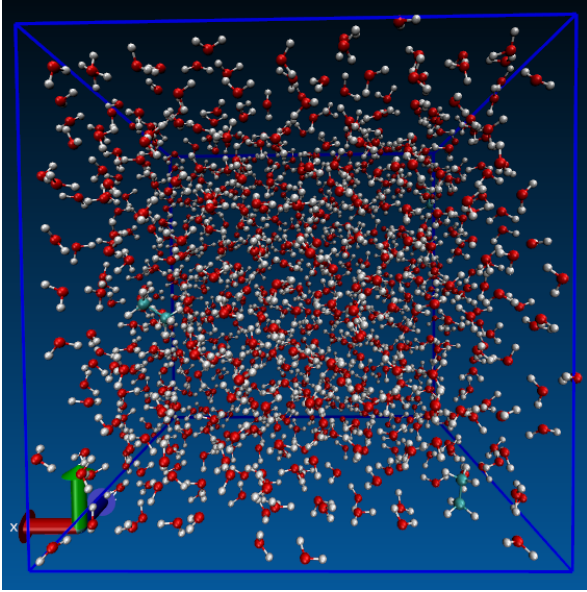


FIG. 3. Structure of ethane-water system after equilibration

TABLE I. Values of simulated temperature (T_{sim}) and density at various coupling temperatures (T_{co}) of propane-water system.

S.N	(T_{co}) K	(T_{sim}) K	$\rho_{sys}(kg/m^3)$	$\rho_w(kg/m^3)$ ^{18,24}
1	283.15	283.144±0.005	993.834±0.043	998.19
2	293.15	293.152 ±0.010	989.386±0.042	997.30
3	297.95	297.949±0.005	986.872± 0.033	--
4	303.05	303.050±0.006	984.104±0.029	--
5	303.15	303.152±0.003	984.051± 0.031	995.61
6	308.25	308.242±0.001	981.093± 0.053	--
7	313.15	313.153 ±0.007	978.44 ± 0.059	994.20
8	315.75	315.753±0.003	976.435± 0.050	--
9	323.15	323.142 ±0.003	971.565 ±0.031	992.17
10	333.15	333.152 ±0.006	964.396 ± 0.048	987.99

Table (I) shows that our simulated value of system density is in maximum deviation of around 1% with that of water density. After equilibration run we perform the production run to calculate the equilibrium properties of the system such as diffusion coefficient

by fixing the number of particles, volume and temperature i.e. NVT ensemble. We use *velocity-rescale* thermostat for this case. We don't couple the system to a fixed pressure and use the structure obtained after equilibration run by which we fix the volume of the system. The production run was carried out for 100 ns with the time step of 2 fs.

C. Energy Profile

Figure (4) represents the energy profile of the butane-water system at 283.15 K with the contributions of different energies. In our force field, total potential energy is the sum of bonded and non-bonded interaction energy. The bonded interaction includes bond stretching, bond angle vibration, proper dihedral, and improper dihedral. The non-bonded interaction includes LJ and coulomb interaction. Intra-molecular non-bonded interactions comprise Coulomb-14 and LJ-14 interactions. Energy profiles, which are variations of energy with time, are used to study the nature of these Lennard-Jones and Coulomb energy. As we have used the cut-off values for Lennard-Jones and Coulomb potential the energy corresponding to them are the short range energies. The total energy is the sum of potential and kinetic energies.

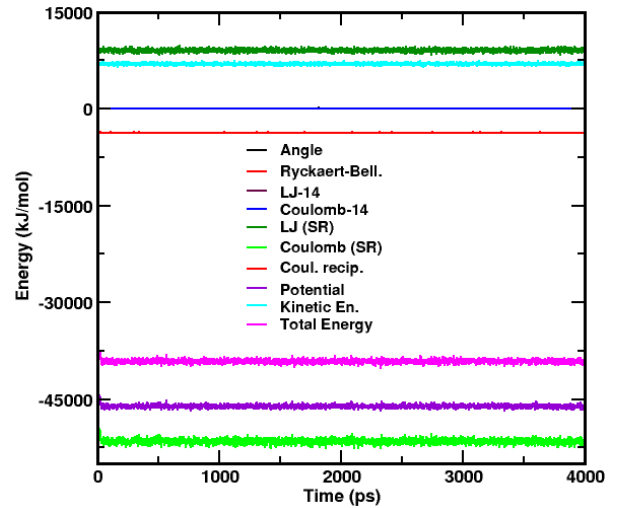


FIG. 4. Energy profile of the butane-water system at $T=283.15$ K.

Looking at the energy profile we can observe that the Coulomb interaction (short range and reciprocal) and LJ interaction have significant contribution to the potential energy of the system while the bonded interaction energies and the pair potential

energies (14-interactions) contribute very less to the potential energy of the system. The Lennard-Jones interaction (LJ-SR and LJ-14) energy is positive and the Coulomb (Coulomb-SR and Coulomb-Recip) energy is negative. The bond angle, LJ-14, Coulomb-14 and Ryckart-Bellman dihedral energies are almost zero. The total potential energy is -46105.70 ± 0.78 kJ mol⁻¹ and the kinetic energy is 6956.73 ± 0.17 kJ mol⁻¹. So the total energy, sum of potential and kinetic energy is -39149.00 ± 0.65 kJ mol⁻¹. The negative value of the total energy shows that the system is bounded and is in stable equilibrium.

IV. RESULTS AND DISCUSSION

In this section, we discuss the structural and dynamical properties of the constituents of the systems.

A. Radial Distribution Function

Radial distribution functions (RDF) were obtained from the simulations, in order to analyse the local structure around the solute and solvent molecule. Radial distribution function (RDF) gives the idea of distribution of neighboring molecules with respect to the reference molecule considered in the calculations. In periodic systems, RDF shows sharp peaks and troughs up to infinity where the separations and heights are the characteristics of the lattice structure. In liquids however, RDF oscillates up to certain orders and then attains constant value as unity²⁵.

We have calculated RDF $g(r)$ of oxygen atoms of water molecules $g_{OW-OW}(r)$, oxygen of water and methyl (CH₃) and methylene (CH₂) carbons of alkanes (methane, ethane, propane, butane) $g_{C-OW}(r)$.

Figure 5(a) represents the RDF of oxygen atoms of water molecules at different temperatures. For the structure of the water molecule, the centre of mass is practically the same as the oxygen centre, which is also the van de Waals sphere centre. This makes the results for the oxygen atom representative of the whole water molecule. The figure explores three different peaks which implies that the molecules are correlated up to third solvation shell. The value of σ for OW-OW is 0.3165 nm, and the van der Waals radius ($2^{1/6}\sigma$) is 0.3553 nm²³. The figure 5(a) shows that excluded region remains fairly independent (0.276 ± 0.002 nm) of changing temperature. It also calculates that the excluded region is smaller than the van der Waals radius which indicates the contributions from other potentials in addition to

the van der Waals potential¹⁸ (see Fig.5b). The first peak position remains at the same position within the error of ± 0.002 nm as a function of temperature. The magnitudes of all the peaks in RDFs decrease on rising temperature. Furthermore, the width of the peaks increases on increasing temperature. Both variations are the consequences of excess volume created in the system and the decrease in co-ordination number with increase in temperature. These results show that the movement of the particles enhances and the solvent becomes less structured as temperature is increased. The figures 5 (a) and that of 5 (b)¹⁸ show that Lennard-Jones plus Coulomb potential covers almost entire potential except many body effects. The second peak and third peak positions of the $g_{OW-OW}(r)$ are 0.450 ± 0.002 nm and 0.680 ± 0.002 nm respectively. These results are in good agreement with the available references^{26,27}. From the simulations, we found that the RDFs between oxygen atoms of water molecules in different alkane-water system are identical in all respects. It showed that the presence of the solute molecule has a negligible effect on the global structure of the solvent.

The RDF between carbon of alkane and the oxygen of water describes solute-solvent interaction. Figure (6) shows the RDF between the methyl (CH₃) and methylene (CH₂) carbons of the alkanes and the oxygen atom of water, calculated from the simulations at 293.15 K. In figure (6), it can be seen that height of the both CH₃ – OW and CH₂ – OW peak clearly decrease with increase in the length of the carbon atoms of the alkane. The methyl carbon groups can always approach the water molecule at closer distances (first peak position ~ 0.38 nm), and the corresponding peaks are systematically more intense than the CH₂ – OW for distances under ~ 0.47 nm. Moreover, the magnitude as well as the excluded regions for g_{CH_3-OW} and g_{CH_2-OW} are different. This is because methyl and methylene carbon do not possess the same partial charge. Furthermore, when oxygen of water (OW) approaches to methyl carbon, it (or the water molecule) also experiences the interactions due to three hydrogens attached to methyl carbon and when oxygen of water (OW) approaches to methylene carbon, it (or the water molecule) experiences the interactions due two hydrogens attached to methylene carbon. This means when OW approaches to these carbons of alkane, it does not exactly experience the same nature of interaction field around methyl and methylene carbon. The combination of these effects suggests that the methyl groups of alkane molecules have a preferential tendency to be dissolved in the vicinity of water molecules and that this tendency decreases with chain length.

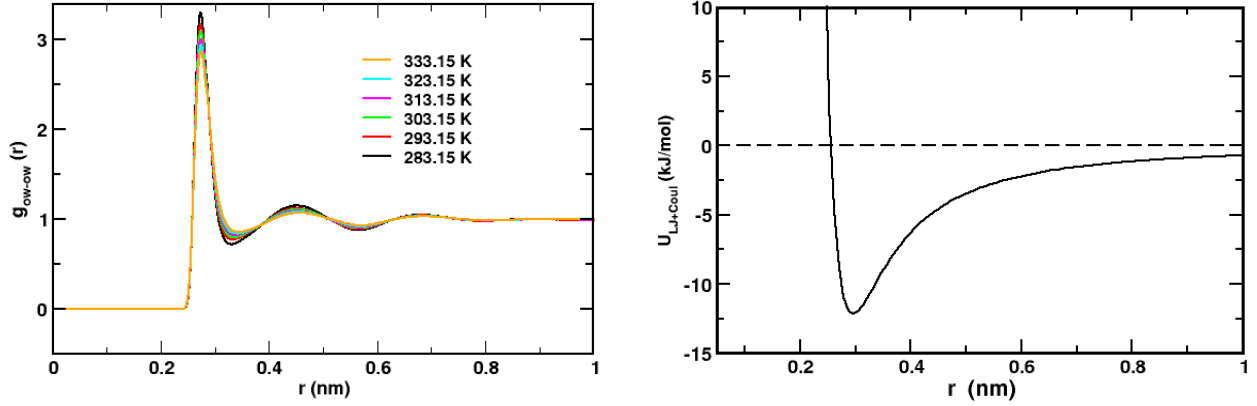


FIG. 5. (a) RDF of oxygen atoms of water molecules at different temperatures (left) (b) Lennard-Jones plus Coulomb ($U_{LJ+Coul}$) potential as a function of distance for two different isolated water molecules¹⁸ (right)

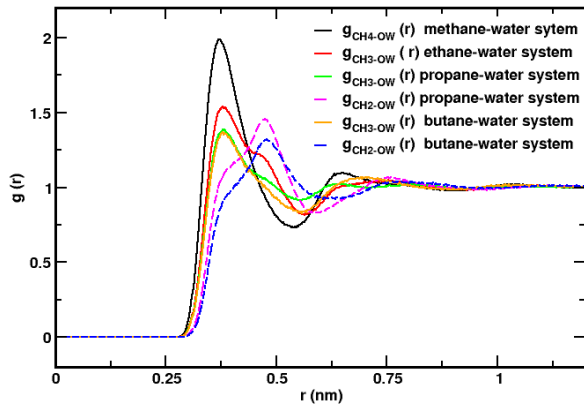


FIG. 6. Radial distribution functions between CH_3 (solid lines) and CH_2 (dotted lines) and oxygen atom of water molecule at 293.15 K.

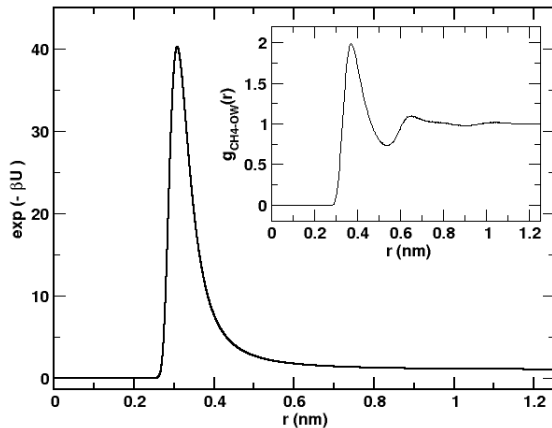


FIG. 7. Plot of exponential of negative of interaction potential between carbon atom of methane and water molecule and the corresponding radial distribution function at 293.15 K.

Fig.7 represents the plot of exponential of negative of Lennard-Jones and Coulomb potential between carbon atom of methane and water molecule as the function of interatomic separation and the corresponding radial distribution function at 293.15 K. The maximum of $\exp(-\beta U)$ (0.31 nm) and the first peak position (FPP) of the corresponding radial distribution function (0.37 nm) are different. This shows that Lennard-Jones plus Coulomb potential doesn't cover almost entire potential.

Furthermore, to obtain the number of interaction sites (N_c) of each type in a coordination shell around the reference site, we have integrated the radial distribution functions (RDFs) as²⁵:

$$N_c = \int_0^{r_{min}} 4\pi \rho g(r) r^2 dr \quad (14)$$

Where r_{min} is the radius of the coordination shell (location of the RDF minima) and ρ is the number density. We have estimated the number of sites of a given groups or molecules around another groups or molecules, as a function of the distance from its centre.

In figure 5, for $g_{OW-OW}(r)$, the peak maxima (r_{max}) of the first shell are obtained at 0.276 nm and the minima (r_{min}) at 0.334 nm for all the alkane-water system. The first shell coordination number was found to be 5.3 ± 0.1 for water molecules. These values or the coordination numbers are in good agreement with the available reference values^{26,27}. The first shell co-ordination number of water molecules around methyl carbon is $n_H \sim 23$, in agreement with the MAS NMR data²⁸. The first cell co-ordination number of water for methylene carbon is greater than that of methyl carbon. This result also suggests that the methyl groups of alkane molecules have a preferential tendency to be dissolved in the vicin-

ity of water molecules. The details of the structural properties with the co-ordination numbers of water molecules around the methyl and methylene carbons of alkane-water system is provided in table II.

TABLE II. Structural parameters from MD simulation of alkane-water system at 293.15 K

system	groups	r_{max} (nm)	r_{min} (nm)	CN
CH4-H2O	CH4-water	0.371	0.542	23.11
C2H6-H2O	CH3-water	0.378	0.565	25.49
C3H8-H2O	CH3-water	0.381	0.555	23.18
C3H8-H2O	CH2-water	0.474	0.588	28.52
C4H10-H2O	CH3-water	0.378	0.558	22.22
C4H10-H2O	CH2-water	0.478	0.606	30.14

B. Diffusion Coefficients

The self-diffusion coefficient of alkane (methane, ethane, propane, butane) and water are calculated by using Einstein's relation (MSD method).

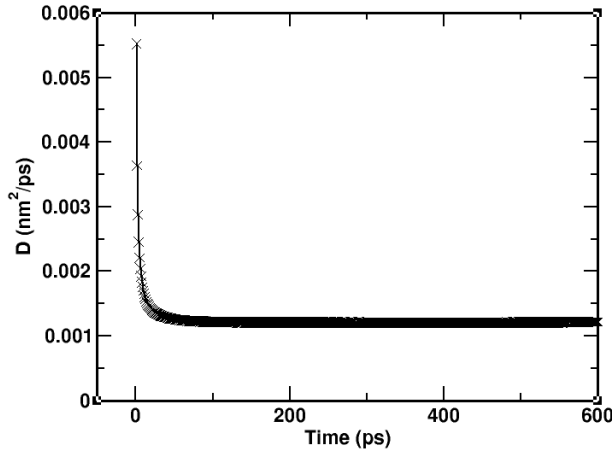


FIG. 8. Plot of Diffusion coefficient ($D = \langle r^2(t) \rangle / 6t$) vs time of ethane at 283.15 K.

The figure (8) shows the variation of diffusion coefficient ($D = \langle r^2(t) \rangle / 6 * t$) with time for ethane at temperature $T = 283.15$ K. Although the production run was carried out for 100 ns, the plots of MSD curve up to 2 ns for all temperatures are portrayed in the graphs. Reason for this is that the MSD curves show approximately a perfect linear nature up to 2 ns and calculated self-diffusion coefficients are promising. Also, from figure (8) we can say that it is reasonable to take time 2 ns while calculating diffusion coefficient as the graph is straight up to 2 ns. At first the diffusion coefficient is high due to ballistic motion and later as time passes it remains

constant. This constant portion of the graph gives the diffusion coefficient¹⁸.

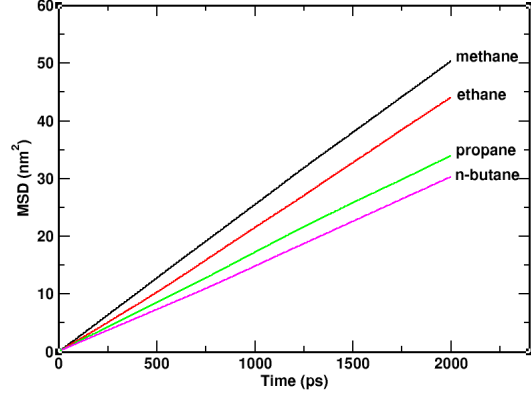


FIG. 9. Plot of MSD vs time of alkane at temperature 333.15 K.

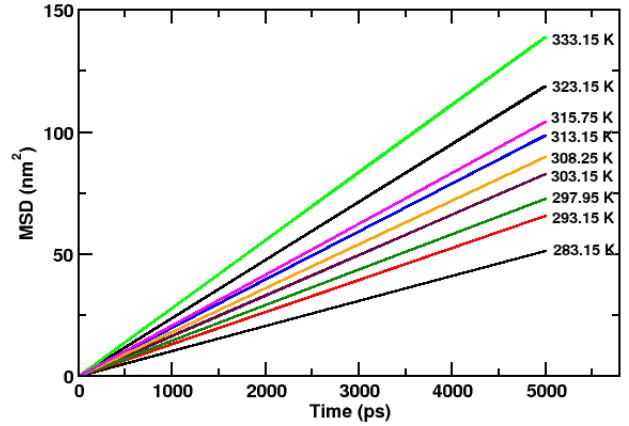


FIG. 10. Plot of MSD vs time of water at different temperatures.

To obtain self-diffusion coefficient of alkanes and water via MSD we plot the graph between mean square displacement with time. Figures (9, 10) show the MSD plot of propane and water at different temperatures respectively. Since the statistics is better due to higher averaging at the starting than towards the ending region, we take the certain portion which has the best statistics. The value of self-diffusion coefficients of the desired species is calculated using equation (2). In our case, we have a simulation time of 100 ns and the best statistics for alkane (methane, ethane, propane and n-butane) molecule is found within 2 ns which can also be justifiable from figure (8) and is very small in comparison to simulation time this is due to lesser number of alkane molecules. For water molecule best statistics is found within 5 ns due to larger number

of water molecules. The binary diffusion coefficient of the alkane-water system is estimated using Darkens relation (Eq.3). Our system consists of 3 alkane molecules (methane, ethane, propane and n-butane each) and 971 water molecules, a separate system, so the mole fraction for alkane is 0.003 and that of water is 0.997. The binary diffusion coefficient is very close to that of self-diffusion coefficient of solute in the mixture due to low solute concentrations studied in this work. The values of self diffusion coefficients of water (H_2O) at different temperatures is presented in the table III.

TABLE III. Self-Diffusion Coefficients of water at different temperatures and the reference experimental values

Temperature (K)	Diffusion Coefficients ($\times 10^{-9} m^2 s^{-1}$)	
	Simulated Value	Experimental Value ²⁹
283.15	1.71	1.54
293.15	2.18	2.02
297.95	2.43	—
303.05	2.70	—
303.15	2.73	2.59
308.25	3.01	—
313.15	3.30	3.24
315.75	3.46	—
323.15	3.95	3.96
333.15	4.64	4.77

The values of the self-diffusion coefficient of alkane (methane, ethane, propane, n-butane) and water obtained from MSD plot and the binary diffusion coefficients along with the references at different temperatures are presented in table (IV).

TABLE IV. The simulated value of binary diffusion coefficient of alkanes (methane, ethane, propane, n-butane) and also the references for them as a function of temperature are listed.

Diffusion Coefficient ($\times 10^{-9} m^2 s^{-1}$)				
System	Temp.(K)	Simulation	Experimental (1) ¹⁴	Experimental (2) ¹⁵
CH4-H2O	283.15	1.79	1.9	—
	293.15	2.08	2.4	—
	297.95	2.35	—	1.88
	303.05	2.56	—	—
	303.15	2.60	3.0	—
	308.25	2.80	—	2.12
	313.15	3.34	4.2	—
	315.75	3.50	—	2.41
	323.15	3.96	4.7	—
333.15	4.36	6.7	—	
C2H6-H2O	283.15	1.29	1.6	—
	293.15	1.54	2.3	—
	297.95	1.66	—	1.52
	303.05	1.89	—	1.59
	303.15	1.90	2.8	—
	308.25	2.18	—	1.72
	313.15	2.32	3.3	—
	315.75	2.45	—	1.95
	323.15	2.84	4.1	—
333.15	3.61	4.9	—	
C3H8-H2O	283.15	0.93	1.3	—
	293.15	1.23	1.8	—
	297.95	1.41	—	1.21
	303.05	1.60	—	1.27
	303.15	1.65	2.4	—
	308.25	1.81	—	1.39
	313.15	1.97	2.7	—
	315.75	2.10	—	1.59
	323.15	2.53	3.5	—
333.15	2.85	4.4	—	
C4H10-H2O	283.15	0.84	0.83	—
	293.15	1.09	1.4	—
	297.95	1.26	—	0.96
	303.05	1.39	—	1.03
	303.15	1.41	1.9	—
	308.25	1.70	—	1.12
	313.15	1.90	2.5	—
	315.75	2.00	—	1.28
	323.15	2.25	3.3	—
333.15	2.58	4.3	—	

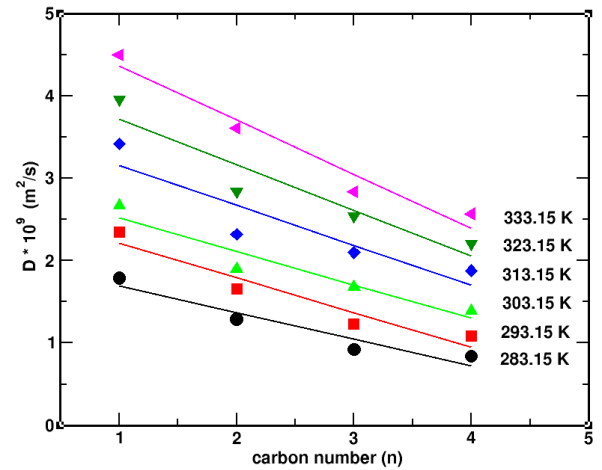


FIG. 11. The variation of simulated values of binary diffusion coefficients of alkanes in water with the numbers of carbon atoms in the alkane chain at different temperatures

Figure (11) shows the variation of binary diffusion coefficients of the molecule with increasing the numbers of carbon atoms of the alkane chain. The diffusion coefficients of the molecules decreases with increasing the number of carbons present in the alkane molecules. Thus, the diffusion coefficients of methane is highest and that of n-butane is lowest.

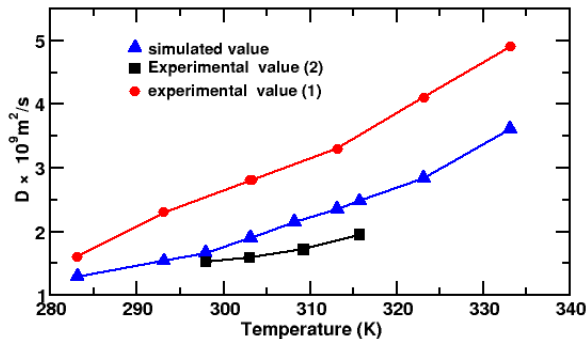


FIG. 12. Simulated and experimental values of binary diffusion coefficients of ethane-water system at different temperatures

Table (IV) shows the self and binary diffusion coefficients of alkane and H₂O molecules from the present work along with the references at different temperatures. The comparison of the values from the table and also from other references explores that self-diffusion coefficients of water from the present work, in general, come in very good agreement with the previous studies^{18,24,29,30}. The experimental and simulated values of self-diffusion coefficients of water in all system are in good agreement with maximum deviation of 11% at 283.15 K²⁹. The simulated values of alkane, on the other hands, show different attitude towards the references. They lie very well in between the experiment performed by (1) D. L. Wise and G. Houghton¹⁴ and (2) P. A. Witherspoon and D. N. Saraf¹⁵. Figure 12 is the comparison of simulated values with the experimental values^{14,15} of binary diffusion coefficients of ethane-water system at different temperatures. They lie very well in between the experimental values^{14,15} within the error of 33%. The deviations of the simulated values with the experimental values follows the same trends in all alkane-water system. There are very large differences in the values of the binary diffusion coefficients reported by them^{14,15}. The diffusion coefficient for both the solute (alkane) and solvent (water) molecules increases with the enhanced temperature, which is due to the increase in the velocity of the molecules, as per relation of the thermal energy with temperature. Furthermore, as the density of the system decreases with increasing temperature, the space available for the alkane molecules to execute

random-walk motion increases³⁰. Finally, based on these facts, the mean squared displacement increases and this change is incorporated by Einsteins relation to yield an increased self-diffusion coefficient.

C. Temperature dependence

Diffusion coefficients of a system generally depends strongly on temperature, being low at low temperatures and are found to be increased with increase in temperature. Temperature variations in diffusivity is explained by the Arrhenius formula¹¹.

$$D = D_0 \exp(-E_a/R T) \quad (15)$$

which can be expressed as

$$\ln D = \ln D_0 - E_a/R T \quad (16)$$

where, D_0 denotes the pre-exponential factor, also called frequency factor, E_a is the activation energy for diffusion, T is the absolute temperature, $R = N_A k_B$ is molar gas constant whose value is 8.31 J mol⁻¹K⁻¹. Both E_a and D_0 are called the activation parameters of diffusion. The simulated binary diffusivities of table (IV) have been fitted to Arrhenius-type expression equation (16) by least squares method, the pre-exponential constant D_0 and the activation energy E_a are reported in table (V).

TABLE V. Table for Activation energies and pre-exponential factors for diffusion of various studied system .

system	E_a (kJ mol ⁻¹)	$D_0 \times 10^7$ m ² /s
CH4-H2O	15.13	7.00
C2H6-H2O	16.18	11.86
C3H8-H2O	17.81	18.67
C4H10-H2O	18.38	22.63
H2O	15.59	13.12

Figure(13) shows the temperature dependence of diffusion coefficient of alkane in water. As the simulation data fit to the equation (15), the temperature dependence of diffusion coefficient follows Arrhenius behavior. From figure (13), it is seen that the diffusion coefficients increase with increase in temperatures. This could be due to the fact that at higher temperature the difference in the density of the system (i.e. alkane and water) and water increases with increase in temperature (see table (I)). Figure (14)

shows the temperature dependence of diffusion coefficient of water in the system containing water and alkane. Figure (14) explicitly shows the temperature dependence of diffusion coefficient of water also follows Arrhenius behavior.

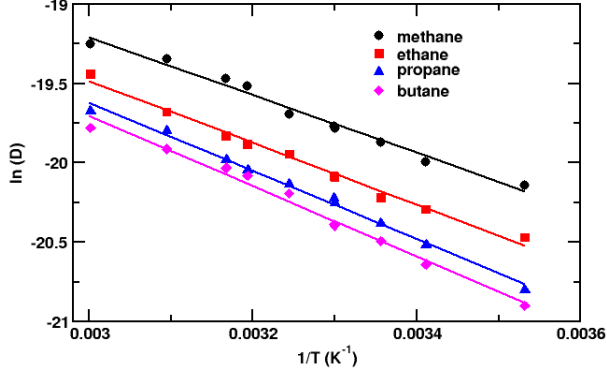


FIG. 13. Arrhenius diagram of the simulated values of binary diffusion coefficients of alkane in water.

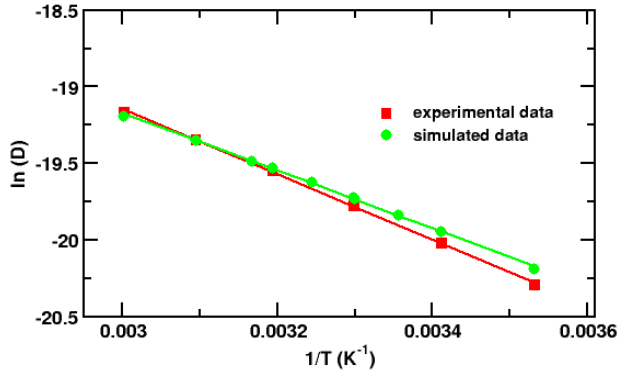


FIG. 14. Arrhenius diagram of the simulated and experimental value of water.

V. CONCLUSIONS AND CONCLUDING REMARKS

In this work, we have computed self diffusion coefficients along with binary diffusion coefficients of the system containing 971 water (H_2O) molecules and 3 alkane (methane, ethane, propane, n-butane) molecules over a wide range of temperatures from 283.15 K - 333.15 K, using molecular dynamics simulation technique. The Extended Simple Point Charge (SPC/E) model of water and Optimized Potential for Liquid Simulations- All Atom (OPLS-

AA) of alkane were used. Here alkane molecule acts as a solute and water (H_2O) as a solvent. The energy profile (figure 4) of the system were studied to know the equilibrium nature of the system.

Structural properties has been studied using Radial Distribution Function (RDF) and co-ordination numbers of the interaction sites has been calculated integrating RDF to the first co-ordination shell. The obtained RDFs show that the system becomes less structured at high temperatures. The equilibrium structural properties of both the components (alkane and water) were studied calculating corresponding radial distribution function (RDF) namely $g_{OW-OW}(r)$ RDF of oxygen atoms of water molecules, $g_{CH_3-OW}(r)$ RDF of carbon atom of methyl group of alkane and oxygen atom of H_2O , $g_{CH_2-OW}(r)$ RDF of carbon atom of methylene group of alkane and oxygen atom of H_2O .

The main aim of our work was to study diffusion phenomenon of the mixture of water and alkane and study its temperature dependence. The self-diffusion coefficients of water and alkane (methane, ethane, propane and n-butane) was estimated using Einstein's method separately. The diffusion coefficients of water are deviated within 11% of the available experimental data²⁹. The binary diffusion coefficient of the system was calculated using Darken's relation. The values of binary diffusion coefficients of alkane in water do not agree well with the experimental values of D. L. Wise and G. Houghton¹⁴ and P. A. Witherspoon and D. N. Saraf¹⁵. It lies in between these two experimental values and the deviation is increasing with increase in temperature. The Arrhenius diagram (plot of natural logarithm of diffusion coefficient vs inverse of temperature) was plotted for self-diffusion coefficients of water and binary diffusion of the alkane-water system separately and it showed temperature dependence of diffusion coefficient of both are of Arrhenius type.

ACKNOWLEDGEMENTS

One of the authors S. Pokharel acknowledges the partial support from the Abdus Salam International Centre for Theoretical Physics, Trieste, Italy through the office of external activities (OEA). Further, A. Subedi, N. Aryal and B. R. Niraula acknowledge the partial financial support from University Grants Commission (UGC), Nepal.

-
- * physicistsupo@gmail.com
† aryaln65@gmail.com
‡ brajnc246@gmail.com
§ arjubedi@gmail.com
¶ npadhikari@gmail.com, npadhikari@tucdp.edu.np
- ¹ R. T. Morrison and R. N. Boyd, *Organic Chemistry*, Pearson, 7th Edition, (2011)
 - ² W. H. Brown and T. Poon, *Introduction to Organic Chemistry*, 5th Edition, John Wiley and Sons, Inc. (2014)
 - ³ J. D. Roberts, and M. C. Caserio, *Basic Principles of Organic Chemistry*, W.A. Benjamin Inc, 2nd Edition, (1977).
 - ⁴ T. A. Weber, *J. Chem. Phys.*, **69**, 2347 (1978)
 - ⁵ D. Frenkel, B. Smit, *Understanding Molecular Simulation From Algorithms to Applications*, Academic Press, U. S. A, (2002).
 - ⁶ M. P. Allen, D. J. Tildesley, *Computer Simulation of Liquids*, Oxford University Press, U. S. A (1989)
 - ⁷ HERMAN J. C. BERENDSEN, *Simulating the Physical World*, Cambridge University Press, (2007)
 - ⁸ Akira Satoh, *Introduction to Practice of Molecular Simulation*, Elsevier, (2011)
 - ⁹ D. C. Rapoport, *The Art of Molecular Dynamics Simulation*, Cambridge University Press, Second Edition, (2004)
 - ¹⁰ O. M. Becker, A. D. MacKerell, Jr., B. Roux, and M. Watanabe, *Computational Biochemistry and Biophysics*, Marcel Dekker, Inc. (2001)
 - ¹¹ H. Mehrer, *Diffusion in Solids*, Springer Series in Solid State Science, Berlin, 155
 - ¹² V. A. Hermandaris, N. P. Adhikari, N. F. A. van der Vegt, K. Kremer, B. A. Mann, R. Voelkel, H. Weiss, Chee Chin Liew, *Macro-molecules* **40**, (2007), 7026-7035.
 - ¹³ N. P. Adhikari, X. Peng, A. Alizadeh, S. Ganti, S. Nayak, S. K. Kumar, *Physical Review Letters* **93**, (2004), 188301
 - ¹⁴ D. L. Wise, and G. Houghton, *Chem. Engng. Sci.*, **21**, 999-1010, (1966).
 - ¹⁵ P. A. Witherspoon and D. N. Saraf, *J. Phys. Chem.*, **69**, 3752, (1965).
 - ¹⁶ P. L. Privalov and S. J. Gill, *Adv. Protein Chem.* **39**, 191 (1988).
 - ¹⁷ C. Kittel and H. Kroemer, *Thermal Physics*, Second Edition, W. H. Freeman and Company, New York (1980).
 - ¹⁸ S. Pokharel, N. Pantha and N. P. Adhikari, *Int. J. Mod. Phys. B* **30** (2016)
 - ¹⁹ V. Ballenegger, S. Picaud, C. Toubin, *Chemical Physics Letters* **432**, (2006), 78.
 - ²⁰ L. S. Darken, *AIME* **175**, (1948), 184
 - ²¹ H. J. C. Berendsen, J. R. Grigera, and T. P. Straatsma, *J. Phys. Chem.*, **91**, (1987).
 - ²² G. A. Kaminski, R.A. Friesner, J. Tirado-Rives and W.L. Jorgensen, *J. Phys. Chem. B* **105**, 6474 (2001).
 - ²³ D. van der Spoel, E. Lindahl, B. Hess, A. R. van Buuren, E. Apol, P. J. Meulenhoff, D. P. Tieleman, A. L. T. M. Sijbers, K. A. Feenstra, R. van Drunen and H. J. C. Berendsen, *Gromacs User Manual version 4.5.6*, (2010).
 - ²⁴ I. Poudyal and N. P. Adhikari, *Journal of Molecular Liquids*, **194**, 77-84, (2014).
 - ²⁵ D. A. McQuarrie, *Statistical Mechanics*, University Science Books, U. S. A, 2000
 - ²⁶ T. H. Gordon and M. E. Johnson, *PNAS*, May 23, 2006, vol. 103, no. 21, 7975
 - ²⁷ T. H. Gordon and Greg Hura, *Chem. Rev.*, 102(8), pp 2651-2670 (2002)
 - ²⁸ C. A. Koh, R. P. Wisbey, X. Wu, and R. E. Westacott, *J. Chem. Phys.* (2000) 113, 63906397
 - ²⁹ A. J. Easteal, W. E. Price and L. A. Woolf, *J. Chem. Soc. Faraday Trans*, **1**, (1989), 85, 1091
 - ³⁰ S. K. Thapa, N. P. Adhikari, *International Journal of Modern Physics B* **27**, (2013), 1350023